INFLUENCES OF BEAM AND COLUMN BAR BOND ON FAILURE MECHANISM

IN REINFORCED CONCRETE INTERIOR BEAM-COLUMN JOINTS

KITAYAMA Kazuhiro *1, TAJIMA Yuji *2, OKUDA Makoto *3 and KISHIDA Shinji *4

ABSTRACT

Reinforced concrete (R/C) interior beam-column joint specimens were tested under the column axial loading and the reversed cyclic lateral loading to study on the joint failure mechanism and the relation between story shear and joint shear. The bond transfer from the beam and column longitudinal bars to surrounding concrete in a joint was important to enhance the story shear. It was judged that the joint core concrete failed by diagonal compression since the compressive principal strain within a joint panel increased with the story drift and exceeded the strain at the concrete compressive strength in cylinder tests. The joint shear force computed from the beam bar forces in which residual tensile forces at the story shear of zero were eliminated on the basis of the measured beam bar strains at beam critical sections decreased with the decrease in the story shear.

KEYWORDS: beam-column joint, bond along beam and column bars, story shear, joint shear, anchorage plate

1. INTRODUCTION

The strength and the failure types in reinforced or prestressed concrete interior beam-column joints were interpreted by Shiohara [1] through the consistent mathematical models without using empirical rules. The paper said as follows. The deterioration of moment resisting mechanism in a beam-column joint, caused by the loss of anchorage ability along the beam longitudinal bars within a joint, results in the joint failure. Both the anchorage capacity along the beam bars passing through a joint and the concrete compressive strength dominate the joint strength. On the contrary, the joint failure type is dominated by the moment resisting capacity in a joint panel or the flexural capacity at the beam critical sections whichever is smaller. Thus the principal factors which settle the strength or the failure type of a beam-column joint are not necessarily coincident with each other. In other words, the joint failure type has nothing to do with the joint input shear force.

Therefore the test results are reported in this paper on the influence of the bond ability along beam and column longitudinal bars passing through a joint on the behavior of R/C interior beam-column joints under earthquake motions. The steel plates were set at beam critical sections to improve the anchorage capacity along beam bars within a joint for three specimens. The additional steel bars were welded to beam longitudinal reinforcement only in a joint for one specimen.

2. OUTLINE OF TEST

2.1 SPECIMENS

*1 Associate Professor, Graduate School of Engineering, Tokyo Metropolitan University, Dr. Eng.
*2 Konoike Corporation, M. Eng.
*3 Kajima Corporation, Tokyo Branch.
*4 Research Associate, Graduate School of Engineering, Tokyo Metropolitan University, Dr. Eng.

Table 1 Properties of specimens and material properties of concrete

Specimen	PB-1	PNB-2	PNB-3	PBU-4
Column Axial Load, kN	883 (Compression, stress ratio:0.33)			
Column Longi. Bars	16-D22			
Beam Longi. Bars	Top: 4-D25, Bottom: 4-D25			
Joint Lateral Bras	2-D10 3 sets			
Anchorage Plates	◯	◯	◯	None
Welded Bars to Beam Bars	None	None	None	◯
Bond along Beam Bars	◯	None	None	◯
Bond along Column Bars	◯	◯	None	◯
Concrete Compressive Strength, MPa	21.0	21.0	21.9	22.2
Concrete Tensile Strength, MPa	2.10	2.38	2.07	2.38
Young's Modulus(*1), GPa	25.1	25.7	26.0	25.8

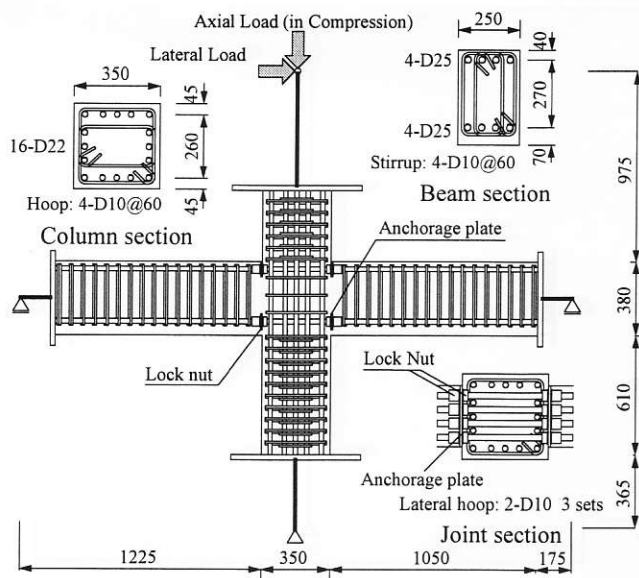*1: Secant modulus at one-fourth of concrete compressive strength

Table 2 Material properties of steel bars

Diameter	Yield Strength, MPa	Tensile Strength, MPa	Fracture Strain, %
D10	404	629	14.0
D22	517	674	17.8
D25	534	685	18.0

Table 3 Material properties of steel plate

Standard	Yield Strength, MPa	Tensile Strength, MPa	Fracture Strain, %
SM490	388	583	20.4

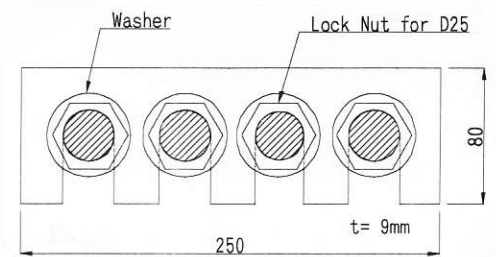Fig. 1 Section dimensions and reinforcement details
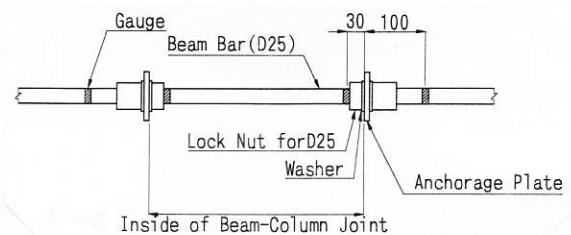

Fig. 2 Detail of anchorage plate

Fig. 3 Anchorage plates and strain gauge locations

Properties of specimens and material properties of concrete are summarized in Table 1. Material properties of steel are listed in Tables 2 and 3. Section dimensions and reinforcement details are shown in Fig. 1. Four plane cruciform subassemblage specimens with one-half scale were tested. Section dimensions and the specified concrete strength (18 MPa) were common for all specimens. The column section was square with 350mm depth. The depth and the width of a beam section were 380mm and 250mm respectively. Three sets of 2-D10 were arranged as the joint lateral reinforcement for all specimens. Test parameter was the bond condition along beam and column longitudinal bars within a joint.

Reinforcing details in a beam-column joint are illustrated in Fig. 4 for all specimens. The anchorage steel plates as shown in Figs. 2 and 3 were placed at the beam critical sections by screwing nuts along beam bars for Specimens PB-1, PNB-2 and PNB-3. These plates were considered to be available for preventing the concrete at beam ends from compressive failure which gives ill effect to the research for the influence of the bond along longitudinal bars within a joint on the behavior of beam-column joints. The bond along beam bars was eliminated within a joint for Specimen PNB-2 by stuffing clay into the dents along deformed bars and wrapping vinyl-sheets. The bond along both beam bars and column bars within a joint was eliminated for Specimen PNB-3 by the same manner as Specimen PNB-2. Deformed steel bars with the diameter of 25mm were welded to each beam bars only in a joint for Specimen PBU-4 in order to increase the sectional area and the perimeter length of beam bars.
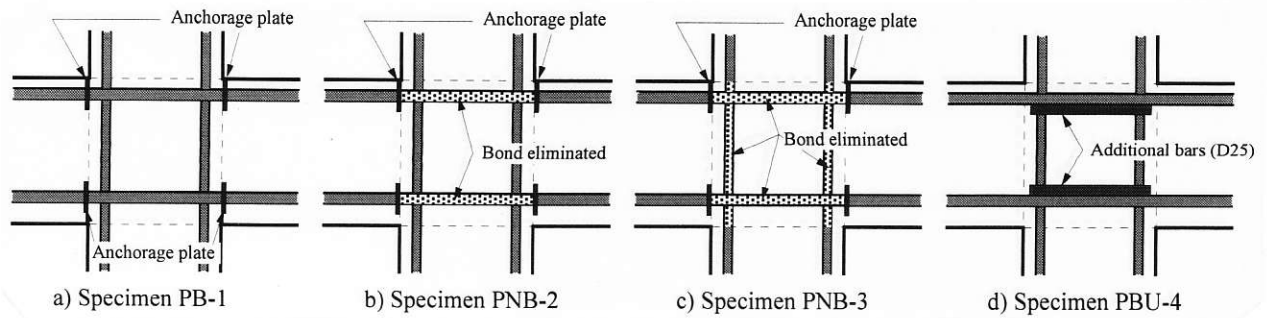
a) Specimen PB-1   b) Specimen PNB-2   c) Specimen PNB-3   d) Specimen PBU-4

Fig. 4 Reinforcing details in joint

(a) Specimen PB-1   (b) Specimen PNB-2   (c) Specimen PNB-3   (d) Specimen PBU-4
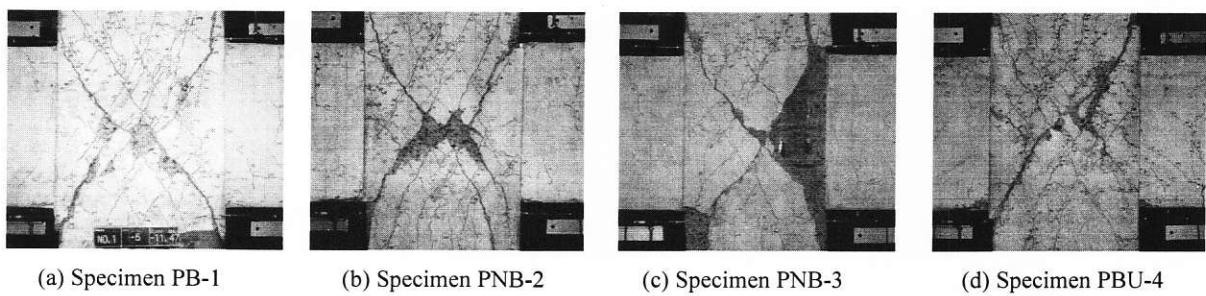
Fig. 5 Crack patterns at story drift angle of 1/33

2.2 LOADING METHOD AND INSTRUMENTATION

The beam ends were supported by horizontal rollers, while the bottom of the column was supported by a mechanical hinge. The reversed horizontal load and the column axial load in constant compression were applied at the top of the column. Specimens were controlled by the story drift angle for one cycle of 1/400, two cycles of 1/200, 1/100 and 1/50 respectively, one cycle of 1/33 and two cycles of 1/25. The lateral force applied to the top of a column, the column axial load and the shear forces of both beam ends were measured by load-cells. A story drift, beam and column deflections, and local displacements of a joint panel were measured by displacement transducers. The strains of beam bars, column bars and the joint lateral reinforcement were measured by strain gauges.

3. TEST RESULTS

3.1 GENERAL OBSERVATIONS

The crack patterns after the story drift angle of 1/33 are shown in Fig. 5. Diagonal shear cracks were observed in a joint panel for all specimens. The crack width along the main diagonal strut in a joint panel expanded dominantly for Specimens PNB-2 and PNB-3 in which the bond transfer along longitudinal bars was removed within a joint. The shell concrete spalled off in a joint panel. The only one of column bars yielded at the story drift angle of 1/25 for all specimens. The beam bars hardly yielded. Therefore it was judged that beams and columns did not yield.
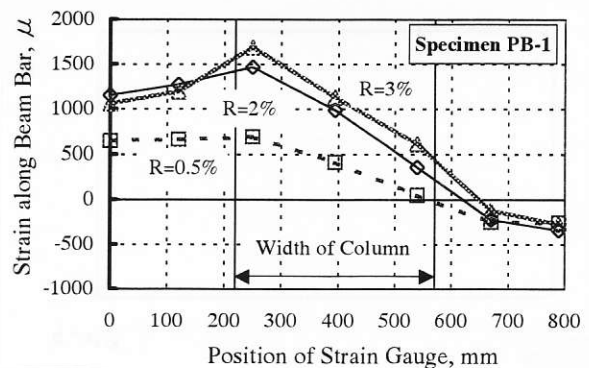

Fig. 6 Strain distribution along beam bar
for Specimen PB-1

The strain distributions along a beam bar are shown in Fig. 6 for Specimen PB-1. Bond along beam bars deteriorated within a joint. However tensile forces of beam bars at a critical section could be developed by the anchorage plate placed at opposite beam critical section for Specimens PB-1, PNB-2 and PNB-3. Then the stress of beam bars within a compressive region at beam end remained compression, resulting in the reduction of concrete compressive force at the beam critical section. Consequently concrete compressive failure at beam ends could be avoided for all specimens.
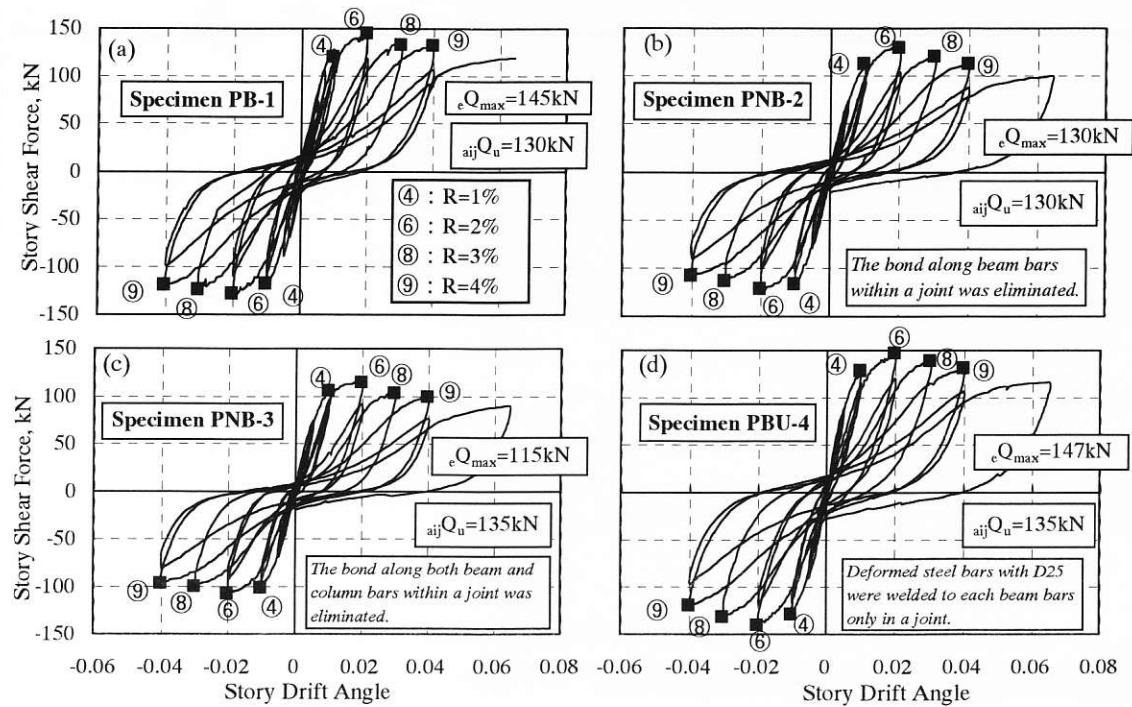
Fig. 7 Story shear force - story drift relations

The contribution of joint shear distortion to the story drift increased with cyclic loading and exceeded the half of the total story drift after story shear force reached at the maximum value. It was concluded on the basis of the research as mentioned above that all specimens eventually failed in joint shear.

3.2 STORY SHEAR - DRIFT RELATIONS

The story shear force – story drift relationships are shown in Fig. 7. The story shear force was computed from moment equilibrium between measured beam shear forces and the horizontal force at the supported point on the top of the column. The story shear reached at the maximum force at the story drift angle of 1/50 and decreased gradually after the drift angle. The maximum story shear for Specimen PBU-4 with twice larger amount of beam bar sectional areas within a joint than other specimens was almost equal to that for Specimen PB-1 with the steel plates for the anchorage of beam bars. The maximum story shear for Specimen PNB-2 where the beam bar bond was eliminated within a joint and Specimen PNB-3, where the bond along both beam and column bars was eliminated, diminished to 89 percent and 79 percent of that for Specimen PB-1 respectively. Therefore the bond ability along beam and column bars within a joint played an important role for the story shear capacity.

The story shear force at joint shear failure computed according to the provisions by Architectural Institute of Japan [2], denoted as $_{aij}Q_u$ in Fig. 7, was smaller than the measured maximum story shear denoted as $_eQ_{max}$ for Specimens PB-1 and PBU-4, which derived conservative estimation. On the contrary, the provisions by AIJ overestimated the measured story shear for Specimens PNB-2 and PNB-3.

Pinching hysteresis loops were obtained for Specimen PBU-4 similarly with Specimen PB-1 although the bond along beam bars within a joint for Specimen PBU-4 was kept good (see Fig. 12) comparing with that for Specimen PB-1. Then the pinching hysteresis shape was caused by shear deterioration in a beam-column joint.

4. DISCUSSION OF TEST RESULTS

Kusuhara and Shiohara [3] proposed that the beam-column joint does not fail in a shear, but fails by the increase in the flexural compression of the concrete at the beam critical section caused by the bond deterioration along beam bars within a joint. Therefore the relationship between the joint shear failure and the transition of a story shear force was investigated. The stresses of beam bars used in the paper were obtained from measured strains by strain gauges through Ramberg-Osgood

Model for the stress-strain relationship for steel.

4.1 JOINT SHEAR - SHEAR DISTORTION ANGLE RELATIONS

The joint shear force was computed in two manners as the following.

a) Tensile force of beam bars was supposed by dividing beam bending moment on a critical section by a constant lever arm length. The joint shear force V_j is obtained by following equation.

$$V_j = \frac{M_{b1}}{j_{b1}} + \frac{M_{b2}}{j_{b2}} - V_c \quad (1)$$

where M_{b1} and M_{b2} are beam bending moments on critical sections, j_{b1} and j_{b2} are lever arm lengths on a beam critical section and V_c is the story shear force. The lever arm lengths were assumed to be the constant value of 7/8 times the beam effective depth.

b) Tensile force of beam bars was computed directly from beam bar stresses at a critical section. The joint shear force is obtained by the equation below.

$$V_j = \sum a_{st} \cdot \sigma_{st} + \sum a_{sb} \cdot \sigma_{sb} - V_c \quad (2)$$

where a_{st} and a_{sb} are the sectional areas of the top and bottom beam bar, σ_{st} and σ_{sb} are the stresses of the beam bar on a critical section computed from the interpolation between stresses measured at two locations close to the beam critical section as depicted in Fig. 3. Equation (2) however may over-estimate joint shear force because stresses of beam bars at both critical sections are enhanced due to the confining action against lateral expansion of damaged concrete within a joint panel. Lateral displacement of the joint panel for Specimen PNB-3 is shown in Fig. 8. There was residual displacement at the story shear of zero after the story drift angle of 1/50. Then the third method to compute joint shear force is indicated below.

Fig. 8 Lateral expansion of joint panel for Specimen PNB-3

c) The schematic stress field in a beam-column joint region is illustrated in Fig. 9 when story shear force returns to zero under reversed cyclic loading. The tensile forces of beam bars at beam critical sections develop as the reaction forces to lateral confinement by framing beams into a joint. The beam tensile forces in this situation do not contribute to the joint shear force as a matter of course. Therefore residual tensile forces should be removed from the beam tensile forces at the peak drift under half cycle of loading when calculating joint shear force as indicated by Equation (3).

$$V_j = \sum a_{st} \cdot \left(\sigma_{st} - \sigma_{to} \right) + \sum a_{sb} \cdot \left(\sigma_{sb} - \sigma_{bo} \right) - V_c \quad (3)$$

Fig. 9 Schematic stress field in joint at story shear of zero

Where σ_{to} and σ_{bo} are the residual tensile stresses of beam top and bottom bars at the story shear of zero just prior to the peak drift.

Joint shear stresses of Specimens PB-1, PNB-2 and PNB-3 obtained by three methods are shown in Fig. 10. The joint shear stress was computed by dividing joint shear force by the effective sectional area of a joint panel that was the product of the average width of the column and beam multiplied by the column depth. The joint shear computed by Equation (2) increased with the increase in joint shear distortion. The joint shear computed by Equation (3), on the contrary, decreased after the story drift angle of 1/25 to the end of the test for Specimen PB-1. The joint shear by Equation (3) was almost equal to that computed by Equation (1) for Specimens PNB-2 and PNB-3 up to the story drift angle of 1/25.
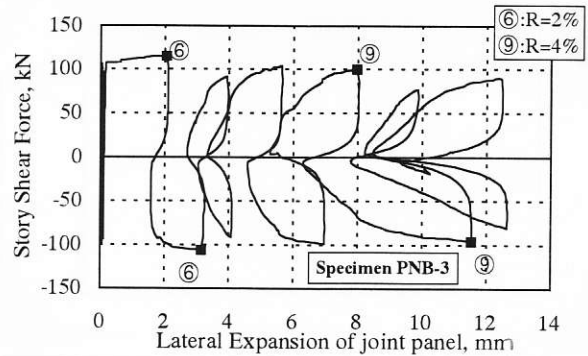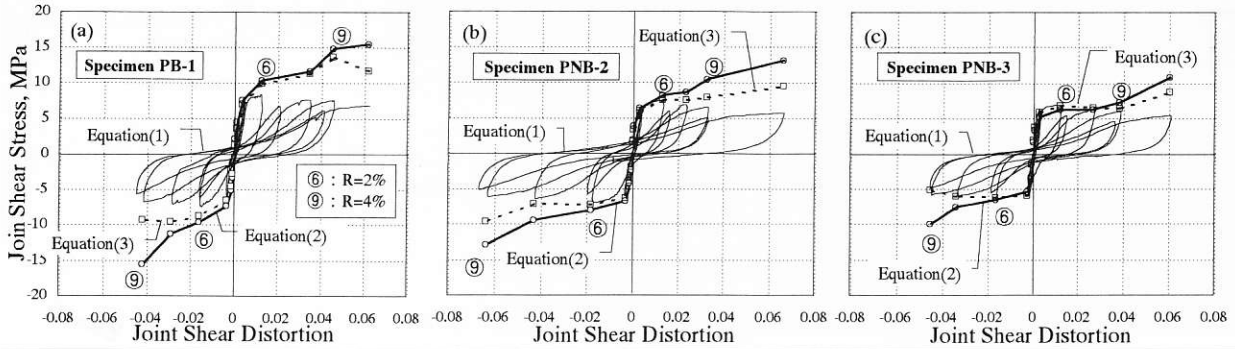
Fig. 10 Joint shear stress - shear distortion relations

4.2 BEAM BAR STRAIN AT CRITICAL SECTION

The beam bar stress within a joint adjacent to a beam critical section for Specimen PB-1 is shown in Fig. 11. Tensile forces of beam bars increased with cyclic loading to the end of the test for all specimens nevertheless the maximum story shear force was attained at the story drift angle of 1/50. The residual tensile force at the story shear force of zero became remarkable after the story drift angle of 1/50 although the strain of beam bars remained to be elastic. It is necessary to take account of residual tensile forces due to damage in a joint core concrete when joint shear force is computed from beam bar forces measured directly.
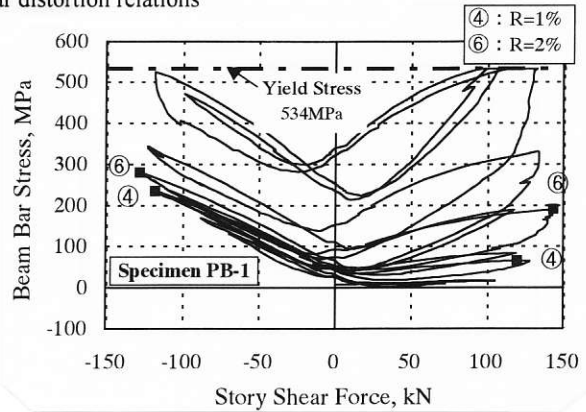
4.3 BOND ALONG BEAM AND COLUMN BARS

The average bond stresses along a beam bar within a joint for all specimens are shown in Fig. 12. The average bond stress was computed by the difference of the pair of beam bar forces adjacent to column faces. Beam bar bond stress for Specimen PB-1 decreased after the story drift angle of 1/50 whereas tensile force of beam bars at critical sections increased to the end of the test. It is judged that the decrease in bond stress along beam bars within a joint resulted from bond deterioration. Beam bar bond stress for Specimen PBU-4 increased up to the story drift angle of 1/25 though story shear force reached at the maximum at the story drift angle of 1/50 and decreased after the drift. Then the decay of story shear resistance was not caused by bond deterioration along beam bars within a joint.
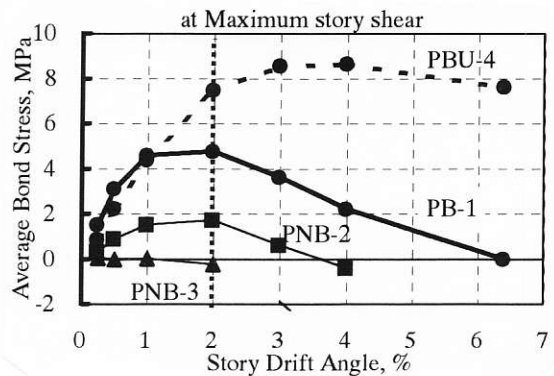
The average bond stresses along a column bar within a joint are shown in Fig. 13. Column bar bond stress reached at the maximum stress of 3 MPa at the story drift angle of 1/50. Bond deterioration along column bars occurred within a joint after the story drift angle of 1/50.

4.4 DEFORMATION IN JOINT PANEL

The lateral and vertical average strains in a joint panel are shown in Figs. 14 and 15 respectively. The tensile principal strain – compressive principal strain relationships in a joint panel are shown in Fig. 16. These strains were computed by using average displacements measured by two horizontal, vertical and

Fig. 11 Beam bar stress adjacent to beam critical section

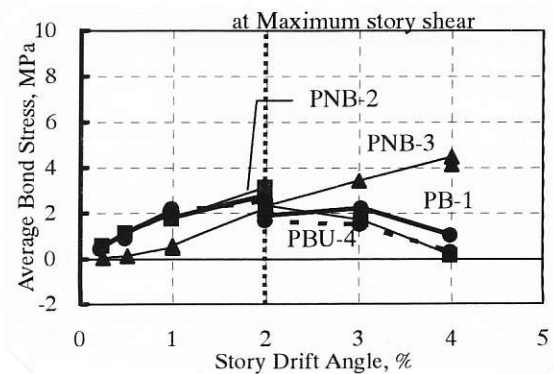Fig. 12 Average bond stress along beam bar within joint

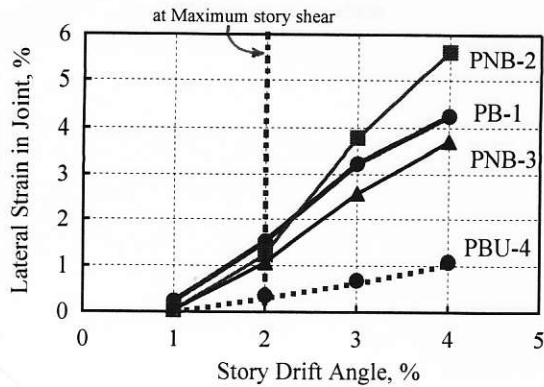Fig. 13 Average bond stress along column bar within joint
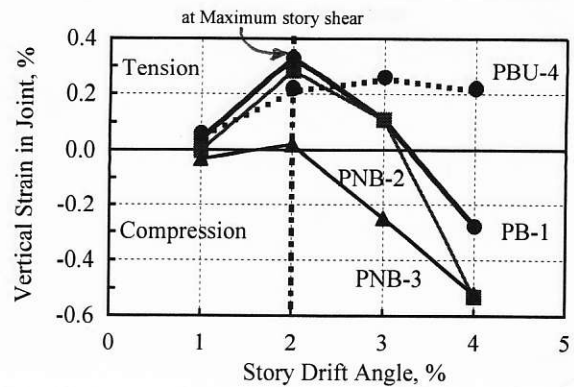
Fig. 14 Lateral average strain in joint panel

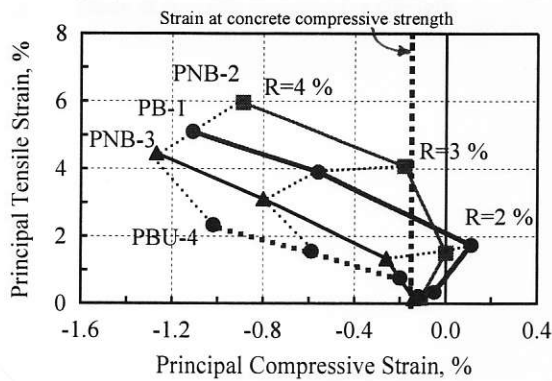Fig. 15 Vertical average strain in joint panel

Fig. 16 Principal strains in joint panel

(a) Specimen PB-1,PNB-2 and PNB-3
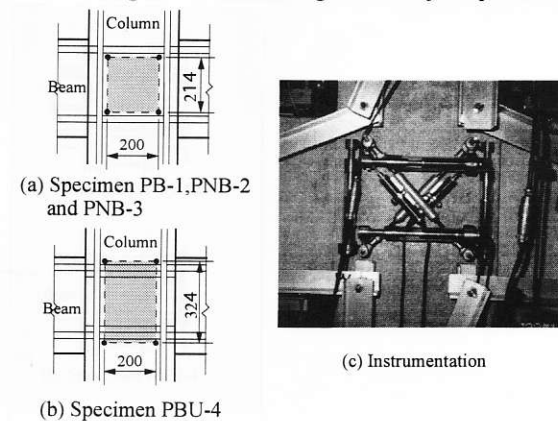
(b) Specimen PBU-4

(c) Instrumentation

Fig. 17 Instrumentation for joint panel distortion

diagonal displacement transducers respectively as illustrated in Fig. 17.

Lateral strains for Specimens PB-1, PNB-2 and PNB-3, where anchorage steel plates were placed at beam critical sections, increased abruptly at the story drift angle of 1/50. On the contrary, lateral strain for Specimen PBU-4 which had the twice amount of beam cross-sectional areas in a joint region comparing with other specimens was smaller than other specimens. Vertical strains of a joint panel changed from elongation to shrinkage at the story drift angle of 1/50 except for Specimen PBU-4. This means that compressive failure in joint core concrete was progressing after the story drift angle of 1/50.

Tensile principal strain in a joint panel augmented suddenly for all specimens at the story drift angle of 1/25 as shown in Fig. 16. The strain in Specimen PBU-4 however was less than the half in other specimens since the lateral expansion of joint core concrete was restricted by beam longitudinal bars passing through a joint with additional welded bars. Compressive principal strain exceeded the strain of 0.16 % at the concrete compressive strength by cylinder tests at the story drift angle of 1/50 for Specimens PNB-3 and PBU-4, at the story drift angle of 1/33 for other specimens. Therefore it is considered that the compressive failure of core concrete took place in a joint panel.

Mohr's strain circles are shown in Fig. 18 at the story drift angle of 1/50 by shaded area, 1/33 by dashed line and 1/25 by solid line to investigate deformation property of a joint panel in more detail. The half angle of inclination of the diameter drawn in the Mohr's circle to the abscissa represents the direction of compressive principal strain to the vertical axis along a column. It means that the larger Mohr's circle is, the severer the damage in a joint core concrete is. The strain circle of Specimen PBU-4 was the smallest among specimens. This indicates that the increase in the cross-sectional areas of beam bars within a joint contributed to restrict joint damage caused by shear. Although bond capacity however was improved simultaneously along beam bars for Specimen PBU-4 as mentioned above, the story shear strength was almost equal to that of Specimen PB-1. This was derived from the following mechanism;
a) compressive principal strain increased beyond the strain of 0.16% at the concrete compressive strength at the story drift angle of 1/50 because isotropic expansion of the joint panel concrete for Specimen PBU-4 was restrained, which can be supposed from the fact that the center of the Mohr's strain circle at the story drift angle of 1/50 was the most adjacent to the point of origin among specimens although the shear distortion angle of 1 % approximately was almost same as other specimens.

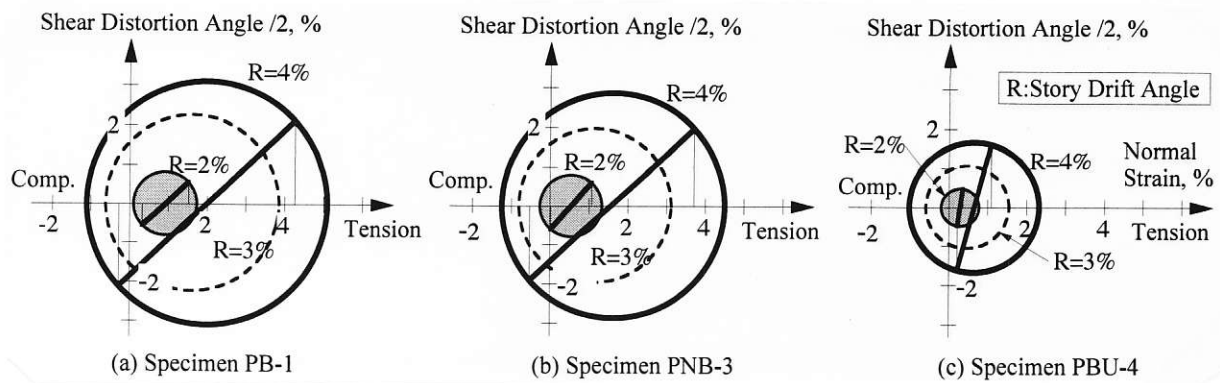(a) Specimen PB-1   (b) Specimen PNB-3   (c) Specimen PBU-4

Fig. 18 Mohr's strain circles for joint panel

b) then the concrete within a joint panel failed uniformly by compression. This was judged from two phenomena. The one is that fine diagonal shear cracks occurred in a joint panel whose direction was 45 degrees approximately for Specimen PBU-4 whereas the direction of other specimens stood up more steeply. The other is that the bond transfer to beam bars within a joint was effective to carry joint shear.

5. CONCLUDING REMARKS

The following conclusions can be drawn from the present study.

1) The story shear capacity of beam-column subassemblages, where the beam bar bond or both the beam and column bar bond was eliminated within a joint, decayed to 89 percent or 79 percent respectively that of control specimen (PB-1). Thus the bond transfer performance along longitudinal bars passing through a beam-column joint provided important influence to story shear capacity.

2) The story shear capacity for Specimen PBU-4, in which bond condition along beam bars was kept good in a joint due to additional deformed bars welded to beam bars, was equal to that for Specimen PB-1 where good anchorage ability was provided to beam longitudinal bars within a joint by steel plates placed at beam critical sections. Joint core concrete failed by compression for both specimens. However the deformation properties as expressed by Mohr's strain circle were fairly different between two specimens.

3) The increase in the amount of beam longitudinal bars only in a joint was effective to delay the progress of concrete damage in a joint panel because additional bars within a joint were useful to confine lateral expansion of joint core concrete. Story shear strength however could not be enhanced because of concrete compressive failure developing simultaneously in a joint.

4) The joint shear stress computed by Equation (2), where tensile forces of beam bars obtained from measured strains at critical sections were used directly, increased successively to the end of the test. On the contrary, the joint shear stress computed by Equation (3), where residual tensile forces of beam bars caused by lateral expansion in a joint panel were considered, decreased or was kept almost constant for some specimens.

ACKNOWLEDGMENT

REFERENCES

(1) Shiohara, H., "Failure Mechanism of Beam-Column Joints," Proceedings for Symposium of "Present or Future Design Method for Prestressed Concrete Structures, " Architectural Institute of Japan, pp.204-239, 2000, (in Japanese).
(2) Architectural Institute of Japan, "Design Guidelines for Earthquake Resistant Reinforced Concrete Buildings Based on Inelastic Displacement Concept," 1999.
(3) Shiohara, H. and F. Kusuhara, "Re-evaluation of Joint Shear Tests of R/C Beam-Column Joints Failed in Shear," Proceedings of the Japan Concrete Institute, Vol.19, No.2, pp.1005-1010, 1997, (in Japanese).